ARGO-YBJ experiment in Tibet

R. Assiro,[1] P. Bernardini,[2 1] C. Bleve,[2 1] A.K. Calabrese Melcarne,[2 1] A. Corvaglia, [1] P. Creti,[1] I. De Mitri,[2 1] G. Mancarella,[2 1] G. Marsella,[3 1] D. Martello,[2 1] M. Panareo,[3 1] L. Perrone,[3 1] C. Pinto,[2 1] A. Surdo,[1] G. Zizzi[2 1] and the ARGO-YBJ Collaboration

[1]Istituto Nazionale di Fisica Nucleare, Sezione di Lecce, Italy

[2]Dipartimento di Fisica, Università del Salento, Italy

[3]Dipartimento di Ingegneria dell'Innovazione, Università del Salento, Italy

The ARGO-YBJ (*Astrophysical Radiation with Ground-based Observatory at YangBaJing*) experiment is a high altitude, full coverage extensive air shower array [1], located at the Cosmic Ray Laboratory of YangBaJing (Tibet, China), 4300 m a.s.l. It is devoted to fundamental issues in astroparticle physics, mainly Cosmic Ray (CR) studies in the $1 \div 1000\ TeV$ range and very high energy (VHE) γ-ray astronomy ($E > 100\ GeV$).

The apparatus (Fig. 1) is a single layer detector logically divided into 154 units called *clusters* ($7.64 \times 5.72\ m^2$), each made by 12 Resistive Plate Chambers (RPCs) operated in streamer mode. Each RPC ($1.26 \times 2.85\ m^2$) is read out by 10 pads ($62 \times 56\ cm^2$), which are further divided into 8 strips ($62 \times 7\ cm^2$) providing a larger particle counting dynamic range [2]. The signals coming from all the strips of a given pad are sent to the same channel of a multi-hit TDC. The whole system provides a single pad time resolution of $\sim 1\ ns$, which allows a complete and detailed three-dimensional reconstruction of the shower front with unprecedented space-time resolution.

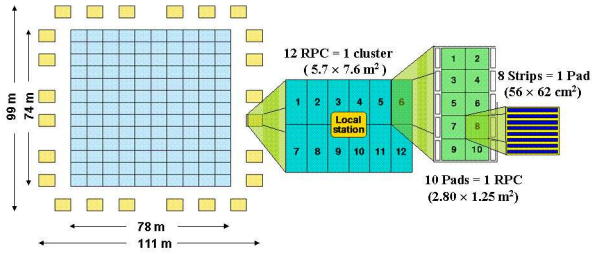

Figure 1. The ARGO-YBJ detector setup. The *cluster* (12 RPCs) is the basic detector and DAQ unit.

The Lecce group contributes to the experiment since its beginning, being strongly involved in development and implementation of the software tools for detector simulation and event reconstruction, in design and production of the electronic devices for the distributed trigger and data acquisition system, in data analysis. Here only the contributions by the Lecce group are presented.

Software tools - *Argo-G* is a FORTRAN program for the full Monte Carlo simulation of the detector, based on the *GEANT3.21* package [3]. It reproduces in detail the detector geometry, the trigger logic and the response to physical processes, including particle interaction with materials, time resolution, inefficiencies, electronics noise, etc. Simulated data are digitized and produced in a format suitable to be analyzed with the same code used for the experimental data.

The reliability of the simulation procedure has been checked and improved by comparing the observables obtained from the Monte Carlo simulation with those from real data. As an example, in Fig. 2 such comparison is made for the strip multiplicity distribution N_{strip} (fired strips in an event), just requiring $N_{strip} \geq 100$ on the central detector (130 clusters) and a reconstructed zenith angle $\theta \leq 40°$.

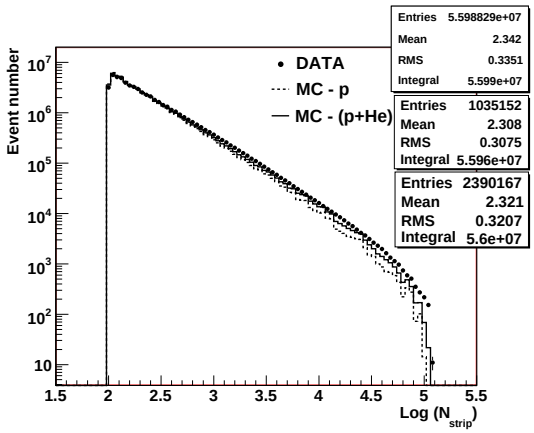

Figure 2. Strip multiplicity distribution from MC compared with the real one. The agreement improves when the He component is added to the pure proton CR primary flux, as expected.

Running with an inclusive trigger requiring at least 20 fired pads in the central detector, the ARGO-YBJ event rate and data flow largely ex-

ceed those of the existing traditional EAS experiments. In order to face out the storage and management of the huge amount of data, *Medea++*, an Object Oriented (OO) reconstruction and analysis program has been written in C++. The OO approach is a powerful tool which allows to store the data as class objects, using a specific software like the ROOT package. This really provides a set of OO structures and functionality allowing the storage and analysis of a large amount of data, including also histograms, graphics and visualization classes.

Medea++ provides the storage of raw (MC and real) data in ROOT structures, the decoding of raw quantities and their conversion into experimental observables. Several algorithms are furthermore implemented for core position and arrival direction reconstruction of the detected showers. A reliable reconstruction of the shower core position up to the edge, and slightly beyond, the active carpet is obtained through a Maximum Likelihood based algorithm, using an *NKG*-like lateral distribution function. Concerning the arrival direction, in the first reconstruction step, the space-time coordinates (positions and times of fired pad in the event) are fitted to a plane. Actually, detailed simulations show that particles within several tens of meters from the shower core form a curved front, which can be well approximated by a conical shape. In a second step, the shower front is thus fitted to a cone, whose axis crosses the core position at ground. As a result, a very good angular resolution is obtained, which obviously depends on the CR primary energy (i.e. detected hit multiplicity).

Electronic devices - The *Local Station* (LS), the basic trigger and data read-out unit of the ARGO-YBJ Data Acquisition System, has been entirely designed and produced by the Lecce group. It collects the shower information, i.e. particle position and arrival time, provided by the RPCs of one cluster. The digital signals from the 80 strips of a single RPC, via the front-end electronics, are sent to a *Receiver* board, so that 12 of such boards are housed in each LS crate (Fig. 3). The logic operations are performed by 11 Programmable Logic Devices (PLD), 10 for the data acquisition and 1 for the board operation and communication control. When receiving a front-end signal, the specific PLD records the active strips and send out a FAST-OR to the TDCs.

Apart the *Receiver* boards, the LS includes also an active *Backplane* and an *In/Out* board. The *Backplane* collects and handles the data provided by the *Receiver* boards. In particular, one section comprises 4 multi-hit, ~ 1 *ns* resolution TDCs, which accept the FAST-OR signals for time measurement. In a different section, 5 FPGA (*Field Programmable Gate Array*) chips calculate the total pad multiplicity in the cluster for trigger purposes. An additional FPGA handles all the operations and prepares the data for the acquisition. When an event trigger occurs, the cluster data are tansferred by the *In/Out* board to the *Central Station*, to be finally registered and stored.

Figure 3. Local Station, entirely designed in Lecce.

In order to extend the energy range up to the "knee region" of the CR spectrum, the read-out of two large size pads (*BigPads*) for each RPC has been implemented (*Analog Read-out System*) [5]. The system unit is the *MiniCrate*, made by 2 sections, each one hosting 3 read-out boards (*Charge Meter Card*, CHM) plus 1 *Control Module* (CM). One *MiniCrate* serves two clusters (thus 24 RPCs and 48 BigPads). The CHM accepts the analog signals and digitizes them through a 12-bit ADC. The CM, designed in the Electronics Laboratory in Lecce, plays an important role in the system, since it (a) supervises the digitization, (b) performs the data reading from 24 ADC channels and their transfer to the connected LS, (c) provides the calibration of each electronic channel, (d) sets the electronic channel amplification gain and the local trigger multiplicity. To generate the calibration pulse, the CM hosts a high speed, 12-bit resolution Digital-to-Analog Converter (DAC).

Timing calibration - The arrival direction of air showers is reconstructed thanks to the times measured by the pixels (pads) of the detector. Assuming a conical front of the incoming particles, the arrival times of the particles are fitted by minimizing the following quantity:

$$\chi^2 = \frac{1}{N_{hit}} \sum_{i=1}^{N_{hit}} w_i \left(t_i - t_0 - \frac{l}{c} x_i - \frac{m}{c} y_i - \alpha r_i \right)^2 \quad (1)$$

This quantity is not a standard χ^2 because the

time uncertainty is neglected. The reconstructed parameters are the direction cosines l, m and the time t_0. The sum is over the fired pads, w_i is the number of strips fired in the i-th pad, t_i is the measured time, x_i, y_i are the pad coordinates and c is the light velocity. The conicity correction depends on the conicity coefficient ($\alpha = 0.1\ ns/m$) and on the pad distance (r_i) to the core in the shower plane.

The presence of systematical time offsets among the read-out channels due to differences in the cable length, in the discharge time in the chambers, in the electronic circuits and so on can invalidate the reconstruction of the arrival directions. Therefore the timing calibration of the detector pixels is crucial in order to get the angular resolution and the absolute pointing accuracy required for the astronomy goals. Because of the large number of pixels (18480 pads in the whole detector) a standard hardware calibration is practically impossible. Therefore an off-line software calibration has been adopted.

We implemented a new method, called Characteristic Plane (CP) method [6]. The secondary particles in the shower are used as calibration beam, which is quasi-parallel to the primary direction. If the primary directions are known, the detector units can be relatively calibrated with a set of shower events. Due to the detector time offsets, there exists a systematic error between the reconstructed primary direction and the true one, which corresponds exactly to the slope of a Characteristic Plane defined by the time offsets of the detector pixels fired by the event. Events firing the same pixels have the same CP, whose direction cosines are exactly the averages of the direction cosines of the event set if the shower azimuth is uniformly distributed. In practice, the CP is estimated by the average over the whole event set. The reconstructed directions of the events are then corrected accordingly and used to calculate the detector time offsets. Finally the time offset of each pixel is averaged over the whole event set.

During the setting-up/debugging phase the calibration procedure has been repeated many times to correct the new time offsets introduced by the change of cables and electronics. Presently the detector is in long-term DAQ for physics run and the calibration stability is checked looking at the changes of the TDC distributions. The calibration updates are not necessary when the hardware is not modified. Typically the calibration is valid for 30-40 days. A detailed description of the calibration procedure is in [7].

The correctness of the procedure was confirmed both by a full simulation and by a hardware sampling calibration. Finally also the Moon shadow analysis and the astronomical observations (see next sections) confirm that the detector is properly calibrated.

Angular resolution and Moon shadow - The pointing accuracy of the ARGO-YBJ detector is checked by means of the Moon shadow. CR are hampered by the Moon, therefore a deficit of cosmic rays in its direction is expected. The size of the deficit allows a measurement of the angular resolution and the position of the deficit allows to evaluate the absolute pointing accuracy of the detector. Almost all the cosmic rays are positive charged and the Moon shadow is bent westward by an angle $1.6^\circ/E(TeV)$ because of the geomagnetic field. Therefore, the Moon shadow shift provides a direct check of the relation between shower size and energy of primary CRs.

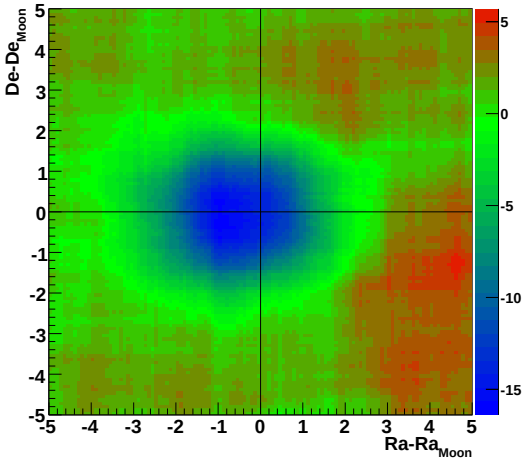

Figure 4. Significance map centered on the Moon. The color scale is in standard deviations.

Fig. 4 shows the deficit significance obtained selecting events with $N_{pad} > 40$ corresponding to a median primary energy of $\sim 4\ TeV$. The maximum significance of the signal is of 16 σ and is found bent westward of 0.37°. The angular resolution obtained from the dimension of the shadow is $1.2 \pm 0.2^\circ$ in good agreement with the estimate obtained with MonteCarlo simulation [9]. It becomes less than 0.6° for $N_{pad} > 200$. The observed shift of the shadow towards West is what expected due to the geomagnetic effect on the protons in Earth-Moon system. This results make us confident about the energy calibration of the detector. Also the Sun shadow has been observed by the ARGO-YBJ detector.

Gamma astronomy - The use of a full coverage detector with a high space-time resolution gives a very detailed image of the shower front. This collection of *images* in the energy range between few hundreds of GeV up to about some hundreds of TeV allows to look for VHE gamma sources [8]. The data collected since November 2007 have

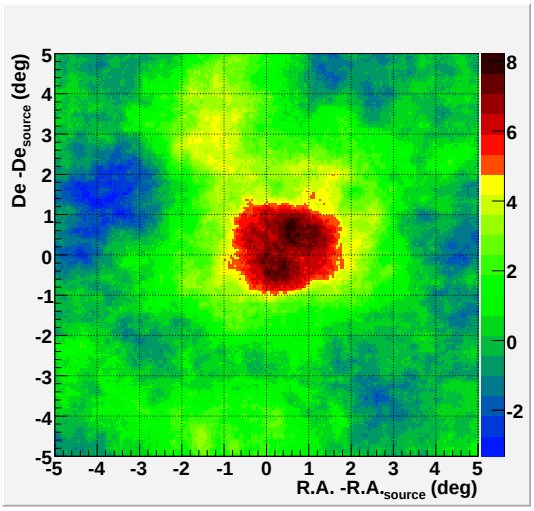

Figure 5. Significance map centered on the Crab Nebula position. The color scale is in standard deviations.

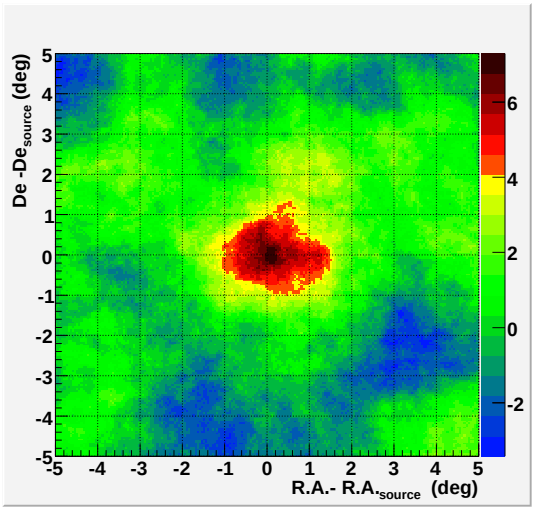

Figure 6. Significance map centered on the Markarian 421 position. The color scale is in standard deviations.

been analyzed looking for signals from Crab Nebula and Markarian 421 (Mkn421). In both cases a significant excess of events has been found.

Fig. 5 shows the excess significance in the Crab Nebula region. It has been obtained selecting events with $N_{pad} > 60$ corresponding to a median gamma energy of $\sim 700\ GeV$. The average number of gamma rays detected per day in the angular window centered on the source is 153 ± 26 using a larger cut ($N_{pad} > 40$). The data can be fitted by the power law spectrum $dN/dE = (4.0 \pm 0.7) \times 10^{-11} E^{-3.0 \pm 0.3}\ \gamma\ cm^{-2} s^{-1} TeV^{-1}$, in fair agreement with other observations

ARGO-YBJ observed Mkn421 from December 13, 2007 to December 23, 2008 for a total of 1965 on-source hours, corresponding to 308 "effective days". The gamma ray flux was variable, with intensity peaks on March, April and June, 2008. In Fig. 6 the excess significance in the Mkn421 region is reported. Also in this case the cut $N_{pad} > 60$ has been applied

In the period February 11 - September 5, the observed average flux was close to the Crab Nebula level. The energy differential spectrum can be fitted by $dN/dE = (2.87 \pm 0.80) \times 10^{-11} E^{-2.77 \pm 0.27}\ \gamma\ cm^{-2} s^{-1} TeV^{-1}$. The observed gamma-ray rate looks correlated with the X-ray rate measured by the All Sky Monitor detector aboard the RXTE satellite, in the $1.5 - 12\ keV$ energy range, as expected by the SSC model [10]. Fig. 7 shows the flare detected in June 2008.

The upper panel shows a stream of images of the sky centered in the Mkn421 location ($E_{50} \sim 700\ GeV$). The flare is maximum in the $4th$ plot. The lower panel shows the event rate as function of the time.

Cosmic ray studies - The high space-time granularity of the ARGO-YBJ detector provides a powerful tool for the study of time structure of EAS front close to the core. Curvature and thickness of the shower front are studied in the energy range from few TeV up to 20 TeV. Details on this analysis can be found in [11]. The digital readout allows detecting shower secondary particles down to very low densities. The time profile of the shower front can be reconstructed by the time of fired pads. Particles within several tens of meters from the shower core are expected to form a curved front. Indeed, to reconstruct the primary particle arrival direction, space-time coordinates (position and time of the fired pads in the event) can be fitted to a cone. A Maximum Likelihood based algorithm is used to perform a reliable reconstruction of the shower core position up to the edge and slightly beyond the active carpet [12]. The pad signals are shaped to 90 ns and sent to a multi-hit TDC so that particles hitting the same pad with a time delay larger than 90 ns are recorded up to a maximum delay of about 1.3 μs.

The space-time structure of extensive air showers depends on primary mass, energy and arrival direction and on the interaction mechanisms with air nuclei. Measurements of shower parameters with several detection techniques would be required for a detailed knowledge of the shower front. A sketch (Fig. 8) illustrates the technique to study an EAS front with a surface detector measuring the particles arrival times and their densities at ground.

Detailed studies of the shower front structure

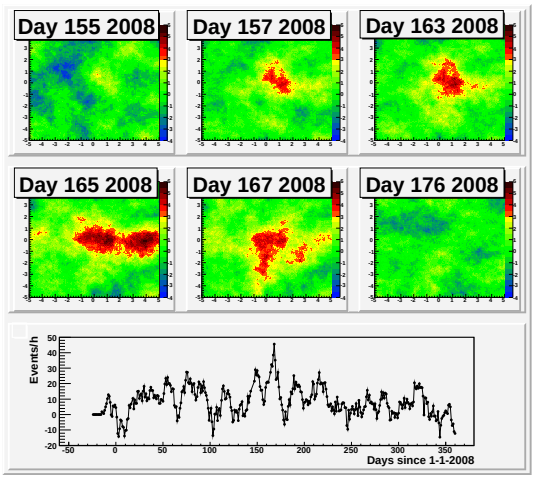

Figure 7. Significance map in the Mkn421 region. The upper panel series illustrates the June flare. The lower panel shows the event rate as a function of time.

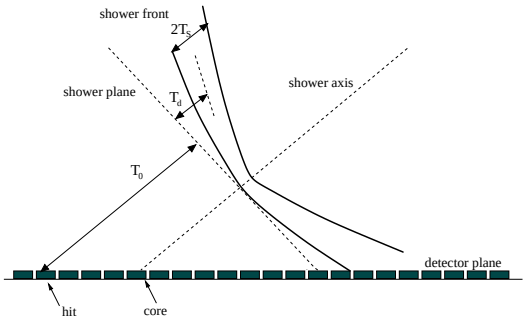

Figure 8. Sketch of shower front geometry and observables

have been carried out by several groups and presented for example in [13–15] and related references.

The features of the ARGO-YBJ detector allow to study the time structure of the shower disk as a function of the distance to the shower axis up to 40 m in 1 m bins. The following observables have been investigated as a function of the distance to the shower axis:

- **the curvature** of the shower front as the mean of time residuals with respect to a planar fit (T_d in Fig. 8)
- **the thickness** of the shower front as the root mean square (RMS) of time residuals with respect to a conical fit (T_S in Fig. 8).

A set of well reconstructed data consisting of about 10^6 events has been selected for this analysis. The reconstructed cores are required to be within an area of $20 \times 20\ m^2$ centered on the carpet. A pad multiplicity greater than 200 is required and a quality cut on the χ^2 (see Eq.1) has been applied in order to reject mis-reconstructed events. A Monte Carlo study demonstrated that these cuts select well reconstructed events with core inside the carpet (contained events) in the energy range between few TeV up to 20 TeV.

Fig. 9 (upper panel) shows the mean of time residuals with respect to a planar fit as a function of the distance to the shower axis for different pad multiplicities ($\theta < 15°$). From simulation of proton primaries it results that, applying the cuts used in this analysis, N_{pad} of 200, 400, 600 and 800 corresponds to average primary energies of about 4, 7, 11 and 15 TeV. The deviation from

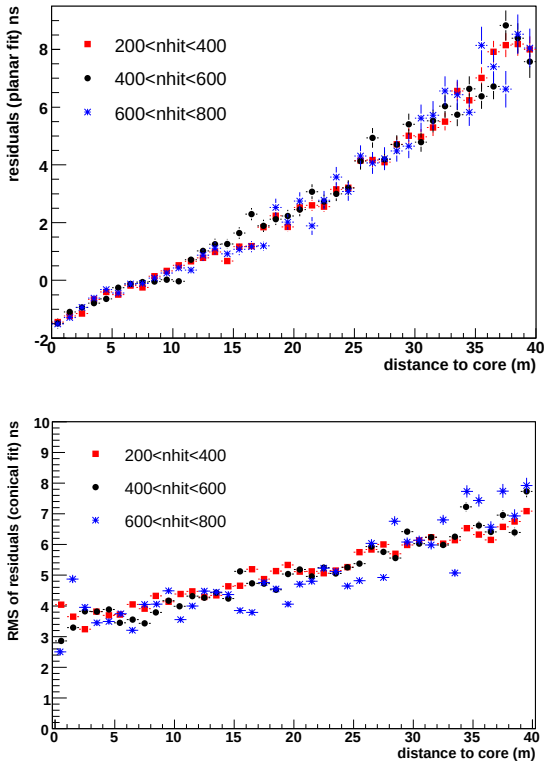

Figure 9. Real data. Mean of time residuals with respect to a planar fit (upper panel) and RMS of time residuals with respect to a conical fit (lower panel) as a function of distance to the shower axis for different pad multiplicities and $\theta < 15°$. Only statistical uncertainties are shown.

a planar fit increases with distance (up to about 8 ns at 40 m) and depends only weakly on pad multiplicity in the considered energy range.

Fig. 9 (lower panel) shows the RMS of time residuals with respect to a conical fit as a function of the distance to the shower axis for different

pad multiplicities ($\theta < 15°$). The thickness of the shower front increases with distance (up to about 7 ns at 40 m) without any significant dependence on pad multiplicity in the considered energy range. Finally, no significant dependence on zenith angle has been observed both for curvature and thickness of the shower front up to 45°.

p-air and p-p cross section measurement - Data analysis for p-air cross section measurement is based on the shower flux attenuation for different zenith angles θ, i.e. atmospheric depths. The detector location (i.e. small atmospheric depth) and features (full-coverage, angular resolution, fine granularity, etc.) ensure the capability of reconstructing showers in a very detailed way. This features have been used to fix the energy ranges and to constrain the shower ages. More details can be found in [16], where some preliminary results are also reported. In particular, different hit (i.e. strip) multiplicity intervals have been used to select showers corresponding to different primary energies. At the same time the informations on particle density, lateral profile and shower front extension have been used to select showers having their maximum development within a given distance/grammage X_{dm} from the detection level. This made possible the unbiased observation of the expected exponential falling of shower intensities as a function of the atmospheric depth through the $sec\ \theta$ distribution. After event selection, the fit to this distribution with an exponential law gives the slope value α, connected to the characteristic length Λ through the relation $\alpha = h_0/\Lambda$. That is:

$$I(\theta) = A(\theta)\, I(\theta = 0)\, e^{-\alpha\,(sec\ \theta - 1)} \qquad (2)$$

where $A(\theta)$ accounts for the geometrical acceptance of each angular bin. The parameter Λ is related to the proton interaction length by the relation $\Lambda = k\lambda_{int}$, where k depends on hadronic interactions and on the shower development in the atmosphere and its fluctuations [17]. The actual value of k must be evaluated by a full Monte Carlo (MC) simulation and it depends on the experimental approach, on the primary energy range and on the detector response.

Therefore the same procedure has been applied to the simulated sample, thus obtaining the value of Λ^{MC}. The value of k, which refers to each strip mutiplicity bin, can then be evaluated as $k = \Lambda^{MC}/\lambda_{int}^{MC}$, where λ_{int}^{MC} is given by the average value of the MC proton interaction length distribution, corresponding to the selected events in the considered multiplicity bin.

The measured interaction lengths are then obtained by correcting the observed lengths, Λ, by the factors k previously determined on the basis of the MC simulation: $\lambda_{int} = \Lambda/k$. Such values must then be corrected for the effects of heavier nuclei in the primary cosmic ray flux. In the present analysis, this has been made by evaluating the contribution to the slope α produced by the addition of a proper helium fraction in the MC simulation, the contribution of nuclei heavier than helium being negligeable. The p-air *production* [18] cross section is then obtained from the relation: $\sigma_{p-air}\ (mb) = 2.41\times10^4/\lambda_{int}\ (g/cm^2)$, while several theoretical approaches can be used to get the corresponding p-p total cross section σ_{p-p} [19].

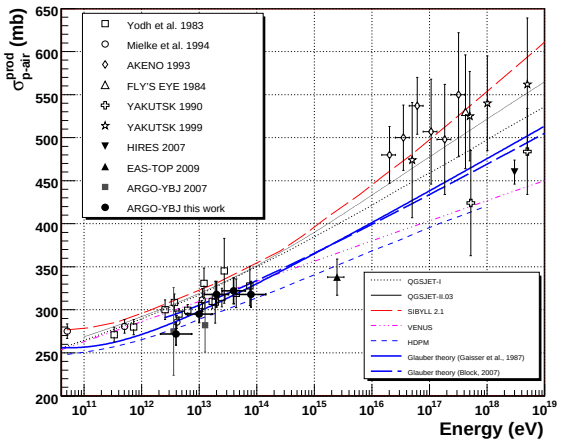

Figure 10. The proton-air *production* cross section as measured by ARGO-YBJ and by different cosmic ray experiments together with the values given by several hadronic interaction models. Also shown are the predictions of two different calculations based on Glauber theory applied to accelerator data.

The analysis was applied to a data sample of about 10^8 events collected by the 130 clusters of the central carpet with a 20 fired pad threshold inclusive trigger. After a first selection based on the quality of the reconstruction, a dedicated procedure was set up in order to reject the background and to constrain the values of X_{dm} (see above).

A suitable simulation chain was used in order to check the effects of the different analysis cuts and have an estimate of the possible systematics. About 10^8 proton initiated and 2×10^7 He initiated showers, were produced by using QGSJET and SIBYLL as hadronic interaction models, while the detector response has been simulated with *Argo-G*.

The measured p-air *production* cross section is reported, in Fig. 10, as a function of the proton energy. The results found by other experiments and the expectations given by some hadronic interaction models are also shown. Even if data are in general agreement, it can be noticed that new results, namely those from ARGO-YBJ, EAS-

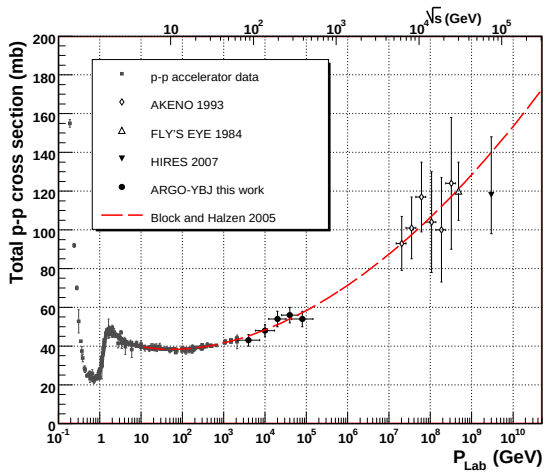

Figure 11. Total p-p cross section (σ_{p-p}) obtained by ARGO-YBJ starting from σ_{p-air}. The same quantity is also shown as published by other CR experiments and measured at accelerator experiments. The dashed line comes from a global theoretical analysis of accelerator data [21].

TOP and HiRes, systematically give cross sections that are slightly lower with respect to the more recent and comprehensive hadronic interaction models actually used in these analyses. The indication for lower cross section (and/or inelasticity) values is also consistent with what found from the analysis of several other EAS observables [20]. The low energy threshold of ARGO-YBJ (with respect to other EAS experiments) allows a direct comparison with the values given by the measurements of unaccompanied hadrons flux, showing a good agreement. This is particularly important since the systematics of the two measurement techniques are completely different. The agreement also extends to the predictions of different calculations based on the Glauber theory, applied to the measurements made at particle accelerators.

The p-p total cross section can be inferred from the measured p-air production cross section as discussed in several papers [19]. In our energy range models differ by less than 10%, this being considered a separate further contribution to the systematic error on σ_{p-p}. Results, for the five energy bins, are summarized in Fig. 11. It can be seen that the ARGO-YBJ data lie in an energy region until now unexplored by accelerator experiments. Our result is in agreement with the general trend of accelerator data showing the rise of the cross section with energy. In particular it is consistent with the asymptotic $ln^2(s)$ behaviour of total hadronic cross sections as obtained in [21].

The Collaboration - The ARGO-YBJ experiment is a Chinese-Italian joint venture with 110 active physicists. Besides the Lecce group, there are six Italian groups ("Tor Vergata" University and INFN, Rome; "Roma 3" University and INFN, Rome; "Federico II" University and INFN, Naple; Torino University and INFN, Turin; Pavia University and INFN, Pavia; Palermo University and Catania INFN, Palermo) and six Chinese groups (Key Laboratory of Particle Astrophyics, Institute of High Energy Physics, Chinese Academy of Science, Beijing; Hebei Normal University, Shijiazhuang, Hebei; Yunnan University, Kunming, Yunnan; Tibet University, Lhasa, Xizang; Shandong University, Jinan, Shandong; South West Jiaotong University, Chengdu, Sichuan).

REFERENCES

1. C. Bacci *et al.* (ARGO-YBJ Collaboration), Astropart. Phys. 17 (2002) 151 and references therein
2. G. Aielli *et al.* (ARGO-YBJ Collaboration), Nucl. Instr. and Meth. in Phys. Res. A 562 (2006) 92
3. GEANT - Detector Description and Simulation Tool, CERN Program Library (1993)
4. R. Assiro *et al.* (ARGO-YBJ Collaboration), Nucl. Instr. and Meth. in Phys. Res. A 518 (2004) 549
5. P. Creti *et al.* (ARGO-YBJ Collaboration), Proceedings of the 29th ICRC, Pune, India (2005)
6. H.H. He, P. Bernardini, A.K. Calabrese Melcarne, S.Z. Chen, Astropart. Phys. 27 (2007) 528, also *physics*/0701291
7. G. Aielli *et al.* (ARGO-YBJ Collaboration), Astropart. Phys. 30 (2009) 287
8. D. Martello (ARGO-YBJ Collaboration), Proceedings of the 30th ICRC, Merida, Mexico (2007)
9. G. Di Sciascio (ARGO-YBJ Collaboration), Proceedings of the 30th ICRC, Merida, Mexico (2007)
10. S. Vernetto (ARGO-YBJ Collaboration), Proceedings of the Gamma 2008 Symposium, Heidelberg Germany (2008), to be published
11. A.K. Calabrese Melcarne, I. De Mitri, G. Marsella, L. Perrone, G. Petronelli, A. Surdo, G.Zizzi (ARGO-YBJ Collaboration), Proceedings of the 30th ICRC, Merida, Mexico (2007)
12. G. Di Sciascio (ARGO-YBJ Collaboration), Proceedings of the 28th ICRC, Tsukuba, Japan (2003)
13. J. Linsley and L. Scarsi, Phys. Rev. 128 (1962) 2384
14. G. Agnetta *et al.*, Astropart. Phys. 6 (1997) 301
15. M. Ambrosio *et al.*, Astropart. Phys. 11 (1999) 437

16. I. De Mitri *et al.*, Proc. ISVHCRI08, Paris 2008, to be published on Nucl. Phys. B (Proc. Suppl.), and references therein.
17. R.Ulrich, (2007) arXiv:0709.1392v1 (astro-ph)
18. R. Engel *et al.*, Phys. Rev. D 58 (1988) 014019
19. See for instance M.M. Block, Phys. Rev. D 76 (2007) 111503 and references therein
20. J.R. Hörandel, J. of Phys. G: Nucl. Part. Phys. 29 (2003) 2439
21. M.M. Block and F. Halzen, Phys. Rev. D 72 (2005) 036006